# Pseudomorphic $In_{0.17}Ga_{0.83}As/Al_{0.32}Ga_{0.68}As$ multiple quantum wells under hydrostatic pressure: Implications for band alignments

R. People, A. Jayaraman, S. K. Sputz, J. M. Vandenberg, D. L. Sivco, and A. Y. Cho
*AT&T Bell Laboratories, Murray Hill, New Jersey 07974*
(Received 17 May 1991)

Photoluminescence from optically pumped strained-layer quantum wells of $In_{0.17}Ga_{0.83}As/Al_{0.32}Ga_{0.68}As$ has been observed under hydrostatic pressures up to 100 kbars, using a diamond-anvil cell. High-resolution x-ray diffraction has been used to determine structural parameters. Analytic expressions have been derived for the hydrostatic-pressure dependence of the $\Gamma$-band-gap photoluminescence intensity for the case of a heterojunction. This allows us to differentiate between two possibilities: whether an observed pressure-induced $\Gamma$-$X$ crossing in a quantum-well structure is indicative of a $\Gamma$ and $X$ crossing in the well material only, or whether the $\Gamma$ band edge in the well material crosses the $X$ band edge of the barrier material. Only in the latter case can information on band alignments be obtained. The present heterostructure is found to satisfy the latter criterion, thus allowing the determination of $\Delta E_v \approx (0.157 \pm 0.025)$ eV, at ambient pressure.

Strained-layer heterostructures containing $In_xGa_{1-x}As$ offer a means to tailor the transport, optical properties, and band alignments in this materials system.[1] In particular, the presence of in-plane compression in pseudomorphic strained layers leads to a reduction in the in-plane (transport) heavy-hole mass[2] and thus enhances the hole mobility. Further, it has been postulated that this same hole-mass reduction should give rise to a reduced density of states thereby allowing the hole quasi-Fermi level to move into the valence band at lower carrier densities, hence reducing the threshold current in strained-layer quantum-well lasers.[3-5] It is also well known that coherency strain can dramatically alter the band alignment in pseudomorphic heterostructures,[6] thus providing an additional degree of freedom in device design. In the present work, strained multiple quantum wells having nominal compositions of $In_{0.17}Ga_{0.83}As/Al_{0.32}Ga_{0.68}As$ have been grown on (001) GaAs using molecular-beam epitaxy. Room-temperature photoluminescence spectra were obtained under hydrostatic pressure generated using a diamond-anvil cell.[7] The pressure medium consisted of a 4:1 volume mixture of methanol and ethanol. The pressure on the sample was monitored using the ruby-fluorescence technique. Photoluminescence was excited using a $Q$-switched and frequency-doubled Nd:YAG laser (peak power of 1 kW and $2 \times 10^{-4}$ duty), analyzed with a 0.5-m-grating spectrometer and subsequently detected using a 7102 photomultiplier. An analysis of the pressure dependence of the photoluminescence intensity of the lowest direct quantum-well transition has allowed us to determine the valence-band offset for the pseudomorphic $In_{0.17}Ga_{0.83}As/Al_{0.32}Ga_{0.68}As$ heterostructure on (001) GaAs.

Hydrostatic pressure, in general, produces a uniform dilation of the center of gravity of a given band edge, and hence a uniform motion (without splitting) of the various semiconductor band gaps (i.e., $\Gamma$, $X$, $L$, etc.). The motion of a gap of given symmetry is defined in terms of the band-gap hydrostatic deformation potential, $(\Xi_d + \frac{1}{3}\Xi_u - a_v)^{(\gamma)}$, and the volume dilation, $\Delta V/V_0$, of the crystal. In general $(\Xi_d + \frac{1}{3}\Xi_u - a_v)$ is negative for $\gamma = \Gamma$ or $L$ and positive for $\gamma = X$.[8] Since $\Delta V/V_0 < 0$ for externally applied hydrostatic pressure, it follows that $\Gamma$ and $L$ band gaps increase in energy whereas $X$-band gaps decrease in energy, under external hydrostatic pressure. The application of hydrostatic pressure to a bulk semiconductor that is direct-gap at ambient pressure can therefore lead to an indirect-gap semiconductor for pressures $P > P_c$ where $P_c$ is that pressure where $\Gamma$ and $X$ conduction-band edges cross.[9-12] This $\Gamma \rightarrow X$ conversion is accompanied by a marked decrease in the $\Gamma$-band-gap photoluminescence intensity for $P > P_c$. In the bulk, the $\Gamma$-band-gap photoluminescence intensity is given by an expression of the form[9-12]

$$\frac{I(P)}{I_0} = \left[1 + A \exp\left[\frac{E_c^{(\Gamma)} - E_c^{(X)}}{k_B T}\right]\right]^{-1} + B \ , \qquad (1)$$

where $I_0$ is a constant proportional to pump intensity and $A \equiv (m_x^*/m_\Gamma^*)^{3/2}(\tau_\Gamma/\tau_X)$. $B = (\tau_{\Gamma-X}/\tau_{\rm rad})$, and represents the probability that an electron at $\Gamma_c$ will undergo a radiative direct transition, rather than an intervalley crossover. In general it is found that $B \ll 1$ except in heavily $p$-type doped bulk layers ($p \gtrsim 2 \times 10^{18}$ cm$^{-3}$) wherein $\tau_{\rm rad}$ is decreased.[11,12] Even at this doping level, Leroux *et al.* found that $B \sim 10^{-4}$ for $p$-type GaAs. Further, extrapolation of the $X$-band gap's pressure dependence from beyond crossover back to zero presure yields the $\Gamma$-$X$ band-edge separation in the ambient bulk. In Eq. (1), $m_\Gamma^*$ and $m_X^*$ are the effective density-of-states electron masses at $\Gamma$ and $X$, respectively; $\tau_\Gamma$ and $\tau_X$ are the recombination lifetimes for electrons at $\Gamma$ and $X$; $\tau_{\Gamma-X}$ is an intervalley scattering time and $\tau_{\rm rad}$ the radiative direct lifetime.

 

In a quantum-well structure under hydrostatic pressure, the observation of a falloff in the photoluminescence (PL) intensity associated with a direct quantum-well transition may be the result of the fact that either (i) the well material has undergone a $\Gamma_c \rightarrow X_c$ conversion to become indirect, or (ii) the well material remains direct but $X_c^B$, the conduction-band edge of the barrier material, crosses $\Gamma_c^W$, the conduction-band edge of the well, thereby causing the quantum well to become indirect both in real space and in momentum space. The latter can only occur if the $X_c$ conduction-band edges of the quantum well exhibit a type-II alignment wherein the $X_c^W$ conduction-band edge of the well material lies at a higher energy than the $X_c^B$ conduction-band edge of the barrier material as shown in Fig. 1(a). If the critical hydrostatic pressures associated with $\Gamma_c \rightarrow X_c$ conduction-band crossing in bulk well and barrier material have been independently determined, then one can immediately determine whether the drop in direct PL intensity from the quantum-well structure is due to effect (i) or (ii). For case (ii) one can obtain information on band alignments, as shown in Fig. 1(b). Various authors[13–17] have used hydrostatic pressure and photoluminescence to determine the band effects in lattice-matched $Al_xGa_{1-x}As/GaAs$ and strained-layer $In_xGa_{1-x}As/Al_yGa_{1-y}As$ multiple quantum wells. In the case of pseudomorphic $In_xGa_{1-x}As/Al_yGa_{1-y}As$ quantum wells on (001) GaAs the $\Gamma_c \rightarrow X_c$ crossover pressure for the $Al_yGa_{1-y}As$ barrier may be readily obtained, however the $\Gamma_c \rightarrow X_c$ crossover for the relaxed barrier materials is not as readily obtainable due to complications associated with both the growth and optical characterization of totally relaxed lattice-mismatched materials. Alternatively, we show that examination of an analytic expression we have derived for the pressure dependence of the heterostructure direct-gap PL intensity allows one to determine whether an observed $\Gamma \rightarrow X$ crossing is indicative of a case-(i) or case-(ii) event.

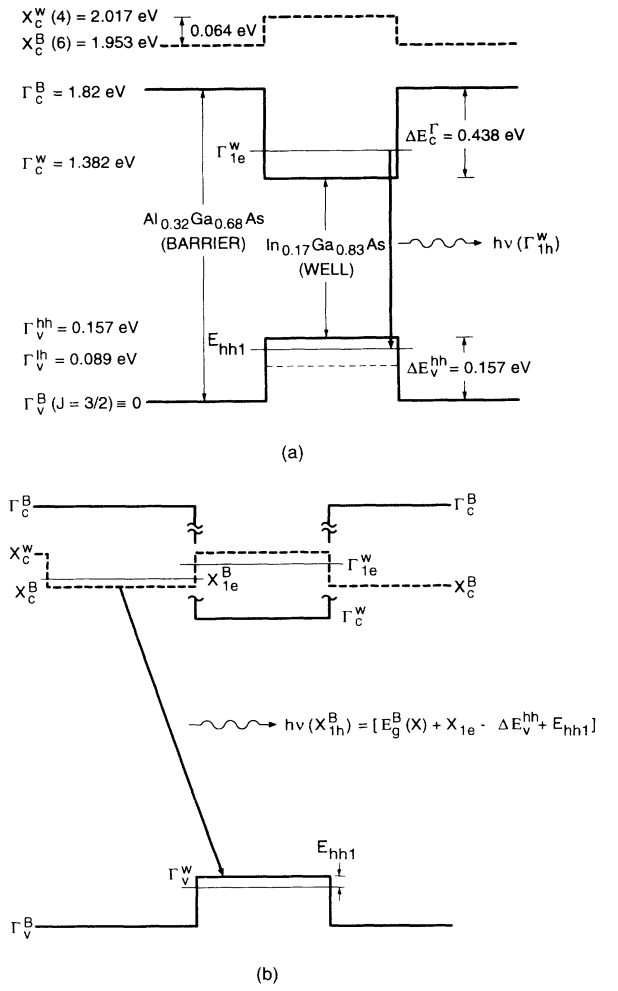


FIG. 1. (a) Band alignments for a quantum well having a type-I alignment for the Γ-conduction bands and type-II alignment for the $X$-conduction bands at ambient pressure ($P=0$). (b) Band lineups for heterojunction in (a) at pressure $P \gtrsim P_c$, the pressure at which the $X_{1e}^B$ electron state in barrier moves below the $\Gamma_{1e}^W$ electron state in the well.

The strained multiple quantum wells studied in the present work were grown using molecular-beam expitaxy on (001) GaAs substrates. The structure consisted of ten periods of $In_xGa_{1-x}As$ strained quantum wells separated by $Al_yGa_{1-y}As$ barriers. The nominal Al concentration in the barrier layers was $y=0.32$, as determined by photoluminescence from a 0.5-μm buffer layer grown before the multiple-quantum-well growths. The In content $x$ in the strained layers was determined using high-resolution x-ray diffraction.[18] A high-resolution scan of the (400) reflection is shown in Fig. 2. The presence of a large number of strong sharp satellite peaks indicates a well-defined superlattice with smooth interfaces and a single period $d$ of 482 Å, which can be calculated from the position of the satellite peaks. The strong asymmetry in the x-ray satellites around the (400) multiple-quantum-well (MQW) peak occurs because of the strain modulation in-

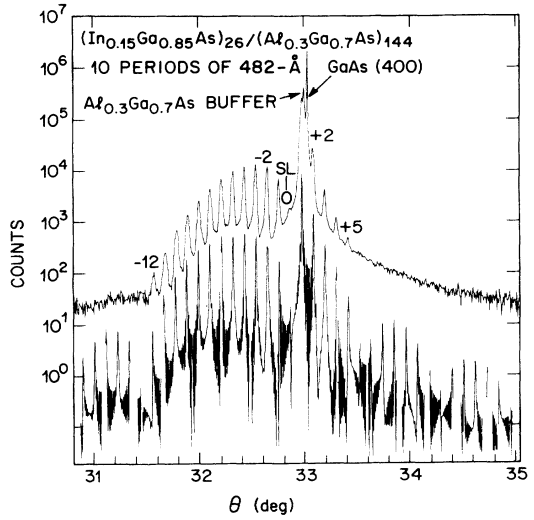


FIG. 2. Upper curve: a high-resolution x-ray scan of the (400) reflection for the present $In_xGa_{1-x}As_{0.32}Ga_{0.68}As$ multiple-quantum-well structure. Lower curve: kinematical simulation for the present structure.

troduced by the accommodation of the large positive mismatch between the $In_xGa_{1-x}As$ wells and the $Al_{0.32}Ga_{0.68}As$ barriers. This large positive tetragonal distortion causes the $(-n)$ satellites to become stronger than the $(+n)$ satellites while the (400) zero-order MQW peak ($n=0$) becomes so weak its position cannot be identified unambiguously. In order to identify the (400) MQW peak and simultaneously determine the structural parameters, the x-ray satellite pattern of the (400) reflection was simulated numerically by using a kinematical step model[19,20] that assumes ideally sharp interfaces. In this model the number of molecular layers $N_W$ and $N_B$ in the $In_xGa_{1-x}As$ well ($W$) and $Al_{0.32}Ga_{0.68}As$ barrier ($B$) and their corresponding lattice spacing $d_W$ and $d_B$ along the [100] direction are the input parameters. The best fit (shown) was obtained for $N_W=26$, $N_B=144$, and $d_W=1.4460$ Å; assuming $d_B=1.4135$ Å, the value for cubic GaAs. These results imply a well thickness $t_W=2d_WN_W=75$ Å, a barrier thickness $t_B=2d_BN_B=407$ Å, and a tetragonal distortion in the quantum well of $\epsilon_\perp^W=(a_\perp^W-a_\perp^B)/a_\perp^B=2.13\%$; $a_\perp^W$ and $a_\perp^B$ being the measured well and barrier lattice parameters along the [100] direction. Multiplying $\epsilon_\perp^W$ by $c_{11}/(c_{11}+2c_{12})$ yields the in-plane compression ($e_\parallel$) for the strained well, which then allows the In content to be deduced using Vegard's law. This procedure yields $x(\text{In})\approx 0.17$.

In Fig. 3 we show observed photoluminescence peak energies versus hydrostatic pressure. The various curves represent least-squares fits to the data. The labels $\Gamma$ and $X$ refer to direct and indirect optical transitions respectively. The subscript $n$ refers to the principal quantum number of the confined states involved in the optical transitions whereas $h$ indicates that the excited electron recombines with a heavy-hole ($h$) valence-band state in the quantum well. The superscripts $W$ and $B$ again denote well and barrier, respectively. The determination that the $X_{1h}^B$ transition (observable for $P\gtrsim 47$ kbars) is associated with a transition from an $X_c^B$-barrier electron to $\Gamma_v^W$-heavy-hole well is of key importance in determining the valence-band offset. The means by which such an assignment has been made is discussed in the following.

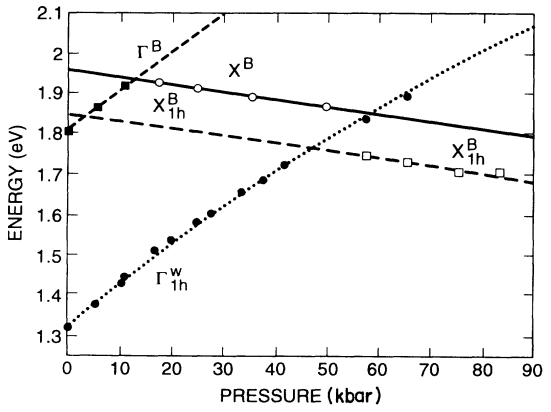


FIG. 3. Pressure dependence of various photoluminescence peaks observed in the present $In_{0.17}Ga_{0.83}As/Al_{0.32}Ga_{0.68}As$ multiple-quantum-well structure. The numeric subscript ($n$) denotes the principal quantum number, and $h$ denotes the heavy-hole character of the final (valence-band) state. The various curves represent least-squares fit to the data, as discussed in the text.

We have investigated the intensity dependence of $\Gamma_{1h}^W$ (lowest-quantum-well direct transition) as a function of hydrostatic pressure in order to determine if the falloff in intensity for $P\gtrsim 47$ kbar can be attriubted to the quantum well converting [case (i)] or if the $X_c^B$-barrier band edge has moved below the lowest ($n=1$) quantum-confined electron state in the well, i.e., case (ii). The pressure dependence of the $\Gamma_{1h}^W$ and $X_{1h}^B$ transitions are well described by $E_g(\Gamma_{1h}^W)=1.328+0.0104P-(2.4863\times10^{-5})P^2$, and $E_g(X_{1h}^B)=1.845-(1.804\times10^{-3})P$, where transition energies are in eV and pressures $P$ in kbars. The observed pressure dependence of the $E_g(\Gamma_{1h}^W)$ photoluminescence intensity is plotted in Fig. 4. The solid line is a best fit to an expression of the form in Eq. (1). The fitting parameters are $A=60$ and $B=0$. Recall that Eq. (1) describes the pressure dependence of the direct-gap photoluminescence intensity for a bulk material. A similar expression applies for the $\Gamma_c\rightarrow X_c$ crossing in a quantum well if the exponent of the $(m_X^*/m_\Gamma^*)$ mass ratio is changed from 1.5 to 1.0 to reflect a two-dimensional density of states. Using $A_{2D}=(m_X^*/m_\Gamma^*)(\tau_\Gamma/\tau_X)$ and well parameters, $m_X^*(In_{0.17}Ga_{0.83}As)=0.83m_0$ and $m_\Gamma^*=0.062m_0$, we find that $\tau_X=0.2\tau_\Gamma$. This applies only *if* the data in Fig. 4 describe conversion of the $In_{0.17}Ga_{0.83}As$ well from direct to indirect for $P\gtrsim 47$ kbars. Note, however, that typically $\tau_\Gamma\approx 1$ ns, and that $\tau_X=0.2\tau_\Gamma$ implies that the band-to-band recombination rate for the well in an indirect configuration exceeds the band-to-band recombination rate in the direct configuration. This can only occur if recombination across the indirect $X$-band gap is controlled by capture into deep traps, which would thereby quench the band-edge luminescence. The fact that we observed strong room-temperature photoluminescence from both $\Gamma$ and $X$-character band gaps clearly precludes this mechanism.

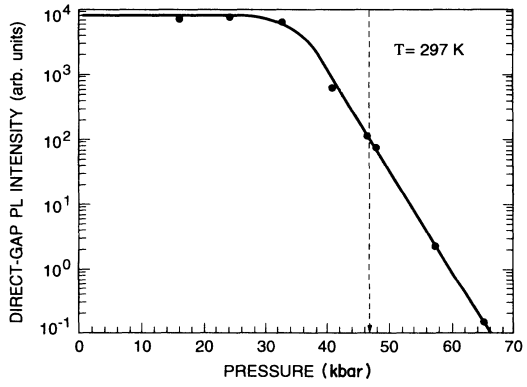


FIG. 4. Pressure dependence of the $\Gamma_{1h}^W$ direct quantum well, photoluminescence intensity. The solid line is a best fit to Eq. (6a).

Since the data in Fig. 4 are not consistent with well conversion only, we consider the possibility that the data may describe a conversion of the type denoted as case (ii), i.e., the $X_c$-barrier state crosses the $\Gamma_c$-well state at $P \approx 47$ kbars. In this case the measured photoluminescence energy at crossover $P=P_c \approx 47$ kbars corresponds to a spatially indirect transition between the $X^B_{1e}$ electron state of the barrier material and the $\Gamma_{1hh}$ heavy-hole state of the well material. Hence from Fig. 1(b), it follows that $E_{\rm PL}(P_c)=[E_g^X(P_c)-\Delta E_v^{\rm hh}+E_{\rm hh1}]$. We have independently measured the barrier $X$-band gap to be 1.88 eV at $P=P_c=47$ kbars and $E_{\rm PL}(P_c)=1.766$ eV, the photoluminescence photon energy at $P_c$. Taking $E_{\rm hh1} \approx 12$ meV we obtain $\Delta E_v^{\rm hh}=0.126$ eV at $P=47$ kbars. This value for $\Delta E_v^{\rm hh}$ is similar to the value of 0.129 eV obtained by extrapolating the difference $(X^B-X^B_{1h})$ to $P=0$ in Fig. 3. Such an extrapolation ignores any pressure dependence of $\Delta E_v$ itself. The valence-band offset at $P=0$ may be estimated by using, e.g., the model solid values[6] for the valence-band deformation potentials, $a_v$. $\Delta E_v^{\rm hh}(P_c)=\Delta E_v^{\rm hh}(0)+\delta[\Delta E_v(P)]$, where

$$\delta[\Delta E_v(P)] \equiv (a_v^B - a_v^W)\Delta V/V_0 = (\delta a_v)(\Delta V/V_0) \ .$$

Using

$$a_v^B = a_v({\rm Al}_{0.32}{\rm Ga}_{0.68}{\rm As}) = 1.580 \text{ eV} \ ,$$

$$a_v^W = a_v({\rm In}_{0.17}{\rm Ga}_{0.83}{\rm As}) = 1.128 \text{ eV} \ ,$$

and

$$-(\Delta V/V_0) \approx P_c/B_0({\rm In}_{0.17}{\rm Ga}_{0.83}{\rm As}) \approx 48 \text{ kbars}/700 \text{ kbars} = 6.85\times 10^{-2} \ ,$$

we get $-\delta[\Delta E_v(P_c)] \approx 0.031$ eV. Therefore, $\Delta E_v^{\rm hh}(0) \approx (0.126+0.031)$ eV $=0.157$ eV. Since the largest uncertainty in the present results occur due to the room-temperature ambient, we estimate

$$\Delta E_v^{\rm hh}(0) = (0.157 \pm 0.025) \text{ eV} \equiv [E_v({\rm In}_{0.17}{\rm Ga}_{0.83}{\rm As}) - E_v({\rm Al}_{0.32}{\rm Ga}_{0.68}{\rm As})]$$

for pseudomorphic growth on (001) GaAs substrate. The resulting band alignment at $P=0$ is shown in Fig. 1(a). Here we have used a strained-alloy band of 1.225 eV as obtained using deformation-potential theory[21] for the bulk well material. The lowest strain-split $X$-band edge of the $In_{0.17}Ga_{0.83}As$ then lies at 1.86 eV in bulk material, assuming an unstrained $X$-band gap of 1.983 eV.[22]

In light of the fact that the fitting parameter describing the data in Fig. 4 does not give information on the ratio of the well band-to-band $\Gamma$ and $X$ recombination times, it is of interest to determine what information can be extracted from a fit to the pressure-dependent photoluminescence intensity $I(P)$ for a heterostructure having band alignments as shown in Fig. 1(a). An expression for $I_{\rm HJ}(P)$ can be derived using phenomenological rate equations for the electron concentrations $n_\Gamma^W$, $n_X^W$, and $n_X^B$ within the $\Gamma$ valley of the well material, the $X$-valley of the well material, and the $X$-valley of the barrier material, respectively. For optical pumping at photon energies $h\nu$, where $h\nu > E_g^B(X)$ but $h\nu < E_g^B(\Gamma)$, the photons are absorbed predominately by the well material. From Fig. 5 we see that the electron concentration in the well material satisfies

$$\frac{\partial n_\Gamma^W}{\partial t} \equiv G_0 - \left[ \left[ \frac{n_\Gamma^W}{\tau_\Gamma^W} \right] + \left[ \frac{n_\Gamma^W}{\tau(\Gamma_c^W \rightarrow X_c^W)} \right] + \left[ \frac{n_\Gamma^W}{\tau(\Gamma_c^W \rightarrow X_c^B)} \right] \right] , \tag{2}$$

where $G_0$ is the optical $e$-$h$ pair-generation rate per unit volume, $\tau_\Gamma^W$ the direct gap recombination time for the well material, $\tau(\Gamma_c^W \rightarrow X_c^W)$ the $\Gamma$-$X$ intervalley electron transfer time in the well material, and $\tau(\Gamma_c^W \rightarrow X_c^B)$ the transfer time for electrons at $\Gamma$ in the well to $X$ in the barrier. Similarly the electron concentration at the $X$ minima in the well material satisfies

$$\frac{\partial n_X^W}{\partial t} \equiv \frac{n_\Gamma^W}{\tau(\Gamma_c^W \rightarrow X_c^W)} - \left[ \left[ \frac{n_X^W}{\tau_X^W} \right] + \frac{n_X^W}{\tau(X_c^W \rightarrow X_c^B)} \right] . \tag{3a}$$

Note that $\tau(X_c^W \rightarrow X_c^B)$ is simply the $X$-valley-electron thermalization time from the $X_c$-valley in the well to the $X_c$-valley in the barrier. Since, as Fig. 1(a) shows, $X_c^W$ is assumed to be higher in energy than $X_c^B$, hence this time is expected to be quite short—on the order of the acoustical-phonon emission time. Hence $\tau(X_c^W \rightarrow X_c^B) \ll \tau_X^W$, the indirect recombination time in the well, so that

$$\frac{\partial n_X^W}{\partial t} \approx \frac{n_\Gamma^W}{\tau(\Gamma_c^W \rightarrow X_c^W)} - \frac{n_X^W}{\tau(X_c^W \rightarrow X_c^B)} \ . \tag{3b}$$

Also,

$$\frac{\partial n_X^B}{\partial t} = \frac{n_\Gamma^W}{\tau(\Gamma_c^W \rightarrow X_c^B)} - \frac{n_X^B}{\tau(X_c^B \rightarrow \Gamma_v^W)} \ , \tag{3c}$$

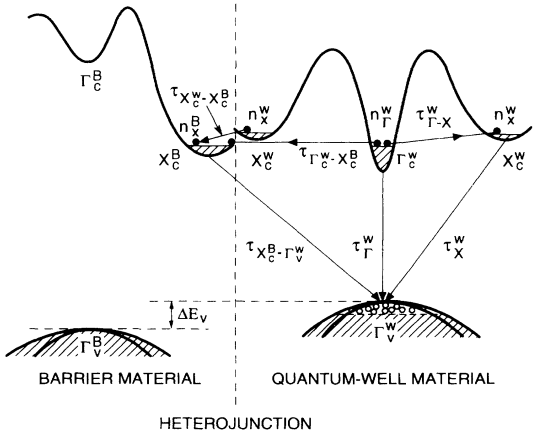


FIG. 5. Schematic of a heterostructure showing electron concentrations $n_X^W$, $n_\Gamma^W$, and $n_X^B$ and the various time constants associated with generation and recombination processes, in our phenomenological model.

where $\tau(X_c^B \rightarrow \Gamma_v^W)$ is the spatially indirect recombination time associated with electron transfer from the $X$-valley of the barrier to the uppermost valence-band edge of the well at $\Gamma$. In the steady state all time derivatives vanish and Eqs. (2) and (3) give

$$G_0 = \left[\frac{n_\Gamma^W}{\tau_\Gamma^W}\right] + \left[\frac{n_X^W}{\tau(X_c^W \rightarrow X_c^B)}\right] + \left[\frac{n_X^B}{\tau(X_c^B \rightarrow \Gamma_v^W)}\right] . \quad (4)$$

The direct photoluminescence intensity from the well material is simply the branching ratio of $(n_\Gamma^W/\tau_\Gamma^W)$ to $G_0$. Therefore

$$\frac{I_{\rm HJ}(P)}{I_0} = \frac{(n_\Gamma/\tau_\Gamma)}{G_0} = \left[1 + \left[\frac{n_X^W}{n_\Gamma^W}\right]\frac{\tau_\Gamma^W}{\tau(X_c^W \rightarrow X_c^B)} + \left[\frac{n_X^B}{n_\Gamma^W}\right]\frac{\tau_\Gamma^W}{\tau(X_c^B \rightarrow \Gamma_v^W)}\right]^{-1} . \quad (5)$$

The electron concentration in the various valleys are given by $n_\Gamma^W = C(T) m_\Gamma^W \exp\{[\phi_n - E_c^W(\Gamma_1)]/kT\}$, where $C(T)$ is dependent only on temperature, $m_\Gamma^W$ is the 2D density-of-states electron mass at $\Gamma$, $E_c(\Gamma_1)$ is the energy position of the first quantum confined electron state in the $\Gamma$ quantum well, and $\phi_n$ is the electron quasi-Fermi-level. Therefore the pressure dependence of the photoluminescence intensity for a heterostructure having band configurations as shown in Fig. 1(a) is given by

$$\frac{I_{\rm HJ}(P)}{I_0} \approx (1 + A_{\rm HJ} \exp\{[E_c^W(\Gamma_1) - E_c^B(X_1)]/kT\})^{-1} . \quad (6a)$$

Note that $E_c^W(\Gamma_1)$ and $E_c^B(X_1)$ now refer to the energies of the lowest quantum confined electron state at $\Gamma$ in the well material and at $X$ in the barrier material, respectively. Note further that at $P = P_c$, where crossing occurs, $E_c^W(\Gamma_1) = E_c^B(X_1)$; however, this does not imply an equality of barrier and well band gaps. Rather, $E_g^{(B)}(X) = E_g^W(\Gamma) + \Delta E_v$ at $P = P_c$, as can be seen from Fig. 1(b). The coefficient $A_{\rm HJ}$ in (6a) is given by

$$A_{\rm HJ} \equiv \left[\frac{m_X^B}{m_\Gamma^W}\right]\left[\frac{\tau_\Gamma^W}{\tau(X_c^B \rightarrow \Gamma_v^W)}\right]\left[1 + \left[\frac{m_X^W}{m_X^B}\right]\left[\frac{\tau(X_c^B \rightarrow \Gamma_v^W)}{\tau(X_c^W \rightarrow X_c^B)}\right]\exp(-\{[E_c^W(X) - E_c^B(X_1)]/kT\})\right] . \quad (6b)$$

For the present heterostructure $E_c^W(X) - E_c^B(X_1) \approx 0.064$ eV, as seen in Fig. 1(a). Therefore the exponential factor in $A_{\rm HJ}$ is $e^{-2.56} \approx 7.73 \times 10^{-2}$ at room temperature. Further, the spatial and momentum indirect recombination is expected to be quite long. In general, $\tau(X_c^B \rightarrow \Gamma_v^W) \sim \tau_X^W(X_c^W \rightarrow \Gamma_v^W)\exp(\kappa L_W/2)$, where $\tau_X^W$ is the indirect-band gap recombination time for the well only and $\exp(\kappa L_W/2)$ arises from the probability of finding the evanescent $X_c$-barrier electron at the center of the quantum well. [Recall that the $X$-conduction-band edges are assumed to have a type-II alignment, as is shown in Fig. 1(a).] The inverse decay length $\kappa = (2m_x^*/\hbar^2)[E_c^W(X) - E_c^B(X_1)]^{1/2} \approx 1.26 \times 10^7\,{\rm cm}^{-1}$. Given $L_W = 75$ Å, we find that $\exp(\kappa L_W/2) \approx e^{4.71} \approx 1.11 \times 10^2$. The thermalization time $\tau(X_c^W \rightarrow X_c^B) \ll \tau_X^W$ (the indirect recombination time for the well material) and the $X$-electron masses $m_X^B, m_X^W$ are comparable, therefore the second term in Eq. (6b) is dominant. Hence, in the present structure:

$$A_{\rm HJ} \approx \left[\frac{m_X^W}{m_\Gamma^W}\right]\left[\frac{\tau_\Gamma^W}{\tau(X_c^W \rightarrow X_c^B)}\right] e^{-\{[E_c^W(X) - E_c^B(X_1)]/kT\}} .$$

The fitting parameter $A_{\rm HJ}$ for the heterostructure photoluminescence pressure dependence therefore gives information on the ratio of the direct band-gap well recombination time to the $X$-valley electron thermalization time. Using the measured $A_{\rm HJ} = 60$ along with $m_X^W = 0.08 m_0$, $m_\Gamma^W = 0.062 m_0$, and $\exp\{-[E_c^W(X) - E_c^B(X_1)]/kT\} = \exp(-2.56)$, we get

$$\tau(X_c^W \rightarrow X_c^B) \approx 10^{-4} \tau_\Gamma^W . \quad (7)$$

Since $\tau_\Gamma^W \sim 1-10$ ns, we find the $X$-valley well to barrier thermalization time $\tau(X_c^W \rightarrow X_c^B) \sim 10^{-12} - 10^{-13}$ s, which is in good agreement with typical acoustic phonon emission times.[23]

In summary, we have measured the hydrostatic pressure dependence of the photoluminescence intensity and peak emission wavelengths for pseudomorphic $In_{0.17}Ga_{0.83}As/Al_{0.32}Ga_{0.68}As$ multiple quantum wells. A direct comparison of the pressure dependence of the lowest-direct-band-gap emission intensity beyond an observed $\Gamma$-$X$ crossing shows that the observed crossing is not due to conversion of the quantum well only. This result implies therefore the crossing of the $X_1$-electron state in the $Al_{0.32}Ga_{0.68}As$ barrier with the $\Gamma_1$-electron state in $In_{0.17}Ga_{0.83}As$ well, from which we extract a value of $\Delta E_v = (0.157 \pm 0.025)$ eV for this heterostructure. These experimental results are in good agreement with the observations at Wilkinson *et al.*[17] A phenomenological rate equation method has been used to obtain the pressure dependence of the direct-gap photoluminescence (PL) intensity for a quantum-well structure. The model shows that in the present heterostructure the PL-intensity data give a measure of the ratio of the direct-gap recombination time for the well $\tau_\Gamma^W$ to the $X$-valley electron thermalization time (from well to barrier), $\tau(X_c^W \rightarrow X_c^B)$. We find that $\tau(X_c^W \rightarrow X_c^B) \approx 10^{-4} \tau_\Gamma^W$. Given $\tau_\Gamma^W \sim 1-10$ ns, this result implies that $\tau(X_c^W \rightarrow X_c^B) \sim 10^{-12} - 10^{13}$ s, in good agreement with acoustic-phonon relaxation times.

We would like to acknowledge R. G. Maines and Mary Simms for sample preparation. We would also like to thank N. A. Olsson and D. V. Lang for constant encouragement. We have also benefited greatly from discussions with M. Lax.

[1]G. C. Osbourn, Phys. Rev. B **27**, 5126 (1983).
[2]J. E. Schirber, I. J. Fritz, and L. I. Dawson, Appl. Phys. Lett. **46**, 187 (1985).
[3]A. R. Adams, Electron. Lett. **22**, 250 (1986).
[4]J. S. Major, Jr., L. J. Guido, K. C. Hsieh, N. Holonyak, Jr., W. Stutius, P. Gavrilovic, and J. E. Williams, Appl. Phys. Lett. **54**, 913 (1989).
[5]S. D. Offsey, W. J. Schaff, P. J. Tasker, H. Ennen, and L. F. Eastman, Appl. Phys. Lett. **54**, 2527 (1989).
[6]See, e.g., C. G. Van de Walle, Phys. Rev. B **39**, 1871 (1989), and references therein.
[7]A. Jayaraman, Rev. Sci. Instrum. **57**, 1013 (1986), and references therein.
[8]K. J. Chang, S. Froyen, and M. L. Cohen, Solid State Commun. **50**, 105 (1984).
[9]P. Y. Yu and B. Welber, Solid State Commun. **25**, 209 (1978).
[10]H. Müller, R. Trommer, and M. Cardona, Phys. Rev. B **21**, 4879 (1980).
[11]D. Olega, M. Cardona, and M. Müller, Phys. Rev. B **22**, 894 (1980).
[12]M. Leroux, G. Pelous, F. Raymond, and C. Verie, Appl. Phys. Lett. **46**, 288 (1985).
[13]D. J. Wolford, T. F. Kuech, and J. A. Bradley, J. Vac. Sci. Technol. B **4**, 1043 (1986).
[14]U. Venkateswaran, M. Chandrasekhar, and H. R. Chandrasekhar, Phys. Rev. B **33**, 8416 (1986).
[15]M. J. Joyce, M. J. Johnson, M. Gal, and B. F. Usher, Phys. Rev. B **38**, 10 978 (1988).
[16]H. Q. Hou, L. J. Wang, R. M. Tang, and J. M. Zhou, Phys. Rev. B **42**, 2926 (1990).
[17]V. A. Wilkinson, A. D. Prins, D. J. Dunstan, L. K. Howard, and M. T. Emeny, J. Electron. Mater. **20**, 509 (1991).
[18]W. J. Bartels, J. Vac. Sci. Technol. B **1**, 328 (1983).
[19]A. Segmüller and A. E. Blakeslee, J. Appl. Crystallogr. **6**, 19 (1973).
[20]D. B. McWhan, M. Gurvitch, J. M. Rowell, and L. R. Walker, J. Appl. Phys. **54**, 3886 (1986).
[21]See, e.g., R. People, Appl. Phys. Lett. **50**, 1604 (1987).
[22]J. R. Chelikowsky and M. L. Cohen, Phys. Rev. B **14**, 556 (1976).
[23]K. Seeger, *Semiconductor Physics* (Springer-Verlag, New York, 1973 ), p. 183.